PHYSICAL REVIEW B **85**, 180301(R) (2012)

Enhanced radiative heat transfer between nanostructured gold plates

R. Guérout,[1] J. Lussange,[1] F. S. S. Rosa,[2] J.-P. Hugonin,[2] D. A. R. Dalvit,[3] J.-J. Greffet,[2] A. Lambrecht,[1] and S. Reynaud[1]
[1]*Laboratoire Kastler-Brossel, CNRS, ENS, UPMC, Case 74, F-75252 Paris, France*
[2]*Laboratoire Charles Fabry, Institut d'Optique, CNRS, Université Paris-Sud, Campus Polytechnique, RD128, F-91127 Palaiseau Cedex, France*
[3]*Theoretical Division, Mail Stop B213, Los Alamos National Laboratory, Los Alamos, New Mexico 87545, USA*
(Received 27 January 2012; revised manuscript received 7 March 2012; published 24 May 2012)

We compute the radiative heat transfer between nanostructured gold plates in the framework of the scattering theory. We predict an enhancement of the heat transfer as we increase the depth of the corrugations while keeping the distance of closest approach fixed. We interpret this effect in terms of the evolution of plasmonic and guided modes as a function of the grating's geometry.

DOI: 10.1103/PhysRevB.85.180301 PACS number(s): 44.40.+a, 42.50.−p, 68.35.−p

The far-field radiative heat transfer between good conductive metals is very low at room temperature, since they are very good reflectors at the infrared frequencies of blackbody radiation. The radiative heat transfer is enhanced in the near field, due to the contribution of evanescent surface modes.[1–3] Polar materials such as SiO_2 or SiC are in addition favored by the contribution of surface phonon polaritons whose resonance frequencies lie in the infrared.[4] There is an analogous effect for metals arising from the surface plasmon resonances but those lie in the ultraviolet and do not contribute significantly to the heat transfer.[5]

It has been shown recently that the radiative heat transfer can be controlled by nanostructuring the interfaces periodically. When the period d is much smaller than the wavelength λ and the separation distance L, the system can be treated using an effective refractive index for the equivalent homogeneous medium. It has been shown that the induced anisotropy introduces additional modes[6] and also allows modulating the flux.[7] For periods on the order of the wavelength, a full solution of Maxwell equations is needed. The heat transfer between two periodic slabs has been studied within a two-dimensional approximation for p polarization using a finite difference time domain (FDTD) technique.[8] A flux enhancement attributed to the excitation of the structure's modes was found. While FDTD allows modeling complex shapes easily, dealing with bulk three-dimensional (3D) media and accounting for polarization effects has not been achieved so far, to the best of our knowledge.

In this Rapid Communication, we compute the radiative heat transfer between one-dimensional (1D) gold lamellar gratings in the framework of the scattering theory. We do include all propagation directions (the so-called conical diffraction) and all polarization states, which is of critical importance in order to deal quantitatively with cross-polarization effects.[9] The scattering theory is the most successful technique for treating the Casimir effect between bodies at thermodynamic equilibrium.[10,11] The method determines the electromagnetic field in the space between the two bodies in interaction in order to compute the Casimir force in terms of the reflection amplitudes on the two bodies. When the two bodies are not at the same temperature, there is a net flux of energy transferred from the warm body to the cold one. Recently, this heat transfer problem between two bodies kept at different temperatures has also been formulated in terms of the scattering properties of the bodies.[12–15]

In the following, we use the scattering amplitudes which have already been calculated for studying the Casimir interaction between 1D lamellar gratings[16] and deduce the heat flux when the two bodies are at different temperatures. We show that the heat flux is largely enhanced when the corrugation depth is increased while keeping the distance of closest approach fixed. We attribute the heat flux growth to the excitation of guided modes and surface plasmons whose frequencies change with the corrugation depth.

We consider the cavity formed by two gratings separated by a distance of closest approach L measured so as to vanish at contact (Fig. 1). The gratings are aligned and not displaced laterally. We model the gold permittivity with a Drude model $\epsilon(\omega) = 1 - \frac{\omega_P^2}{\omega(\omega+\imath\gamma)}$ with $\omega_P = 9$ eV and $\gamma = 35$ meV. We write the heat flux q between two bodies at temperatures T_1 and T_2 as[3]

$$q = \iiint \left[e_{T_1}(\omega) - e_{T_2}(\omega)\right]\mathcal{T}_L(\mathbf{k},\omega)\frac{d\omega d^2\mathbf{k}}{(2\pi)^3}, \tag{1}$$

where $e_T(\omega) = \hbar\omega(e^{\hbar\omega/k_BT} - 1)^{-1}$ is the mean energy per mode of frequency ω at temperature T, while $\mathcal{T}_L(\mathbf{k},\omega)$ is the sum (trace) of the transmission factors for all the modes of frequency ω and lateral wave vector $\mathbf{k}$ between the two gratings separated by a distance L.[17,18] The expression of this transmission factor is given by scattering amplitudes

$$\mathcal{T}_L(\mathbf{k},\omega) = \mathrm{tr}(\mathbf{D}\mathbf{W_1}\mathbf{D}^\dagger\mathbf{W_2}), \tag{2a}$$
$$\mathbf{D} = (\mathbf{1} - \mathbf{S_1}\mathbf{S_2})^{-1}, \tag{2b}$$
$$\mathbf{W_1} = \mathbf{\Sigma}_{-1}^{pw} - \mathbf{S_1}\mathbf{\Sigma}_{-1}^{pw}\mathbf{S_1}^\dagger + \mathbf{S_1}\mathbf{\Sigma}_{-1}^{ew} - \mathbf{\Sigma}_{-1}^{ew}\mathbf{S_1}^\dagger, \tag{2c}$$
$$\mathbf{W_2} = \mathbf{\Sigma}_{1}^{pw} - \mathbf{S_2}^\dagger\mathbf{\Sigma}_{1}^{pw}\mathbf{S_2} + \mathbf{S_2}^\dagger\mathbf{\Sigma}_{1}^{ew} - \mathbf{\Sigma}_{1}^{ew}\mathbf{S_2}, \tag{2d}$$
$$\mathbf{S_1} = \mathbf{R_1}(\mathbf{k},\omega), \tag{2e}$$
$$\mathbf{S_2} = e^{\imath k_z L}\mathbf{R_2}(\mathbf{k},\omega)e^{\imath k_z L}. \tag{2f}$$

Mode counting is defined over frequency ω and lateral wave vector $\mathbf{k}$ restricted to the first Brillouin zone, due to the Bloch theorem. $k_z = \sqrt{\omega^2/c^2 - \mathbf{k}^2}$ is the longitudinal wave vector for the Fabry-Pérot cavity, with the principal square root used in its definition $-\frac{\pi}{2} < \arg k_z \leqslant \frac{\pi}{2}$. The operators $\mathbf{\Sigma}_n^{pw/ew} = k_z^n\mathbf{\Pi}^{pw/ew}$ involve the projectors $\mathbf{\Pi}^{pw/ew}$ on the propagative

 ©2012 American Physical Society

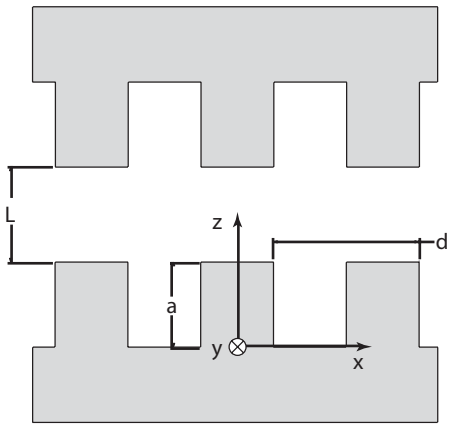

FIG. 1. The conventions used in the present article. The grating period is d, the corrugation depth is a, and the distance of closest approach of the two gratings is L. The lines of the grating are along the y direction, while the Fabry-Pérot cavity between the two gratings is along the z direction.

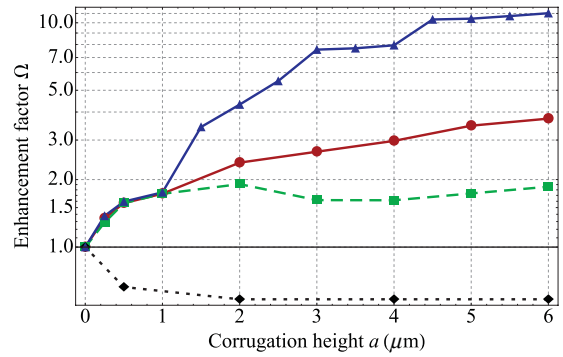

FIG. 2. (Color online) The enhancement factor Ω between two gold gratings as a function of the depth a of the corrugations, with the distance of closest approach kept fixed $L = 1$ μm. Blue solid curve (triangles): period $d = 1$ μm. Red solid curve (circles): period $d = 2.5$ μm. Green dashed curve: period $d = 10$ μm. Black dotted curve: proximity approximation.

or the evanescent sector, respectively. $\mathbf{S_1}$ and $\mathbf{S_2}$ are scattering operators defined from the reflection operators $\mathbf{R_1}(\mathbf{k},\omega)$ and $\mathbf{R_2}(\mathbf{k},\omega)$. $\mathbf{S_i}$ are represented in the basis of the wave vectors $\{\mathbf{k}^{(n)}\}$ coupled by the grating. We define $\mathbf{k}^{(n)} = \mathbf{k} + n\frac{2\pi}{d}\hat{\mathbf{e}}_x$ where d is the grating period, $\hat{\mathbf{e}}_x$ the direction perpendicular to the lines of the grating (see Fig. 1), and n runs from $-N$ to $+N$, where N is the highest diffraction order retained. The operators $\mathbf{S_i}$ are square matrices of dimension $2(2N+1)$ (Ref. 16) as well as all bold operators appearing in Eqs. (2). All scattering operators appearing in Eqs. (2) are represented in the (s/p) (also denoted TE/TM) polarization basis, well adapted to propagative fields. The reflection operators are calculated following the rigorous coupled-wave analysis (RCWA) method described in Ref. 19: The fields are expressed in terms of a Rayleigh expansion in both homogeneous regions $z < 0$ and $z > a$. In the corrugated region $0 > z > a$, the fields are developed in Fourier components. The Maxwell equations are solved in each region and writing the continuity of each Rayleigh and Fourier components at the boundaries $z = 0$ and $z = a$ leads to the reflection and transmission coefficients for the grating. In the limit of an infinite number of Fourier harmonics, this method solves exactly the diffraction of the fields by the grating. Metallic gratings are known to be difficult to account for using the RCWA method. We incorporate in the RCWA formalism the modifications presented in Ref. 20 which greatly improve the convergence rate for the reflection coefficients of a p-polarized light impinging on a metallic grating, and our calculations are performed with $N = 51$ which shows converged results.

In the following, we apply formula (1) to compute the heat transfer coefficient h defined as $h = \frac{q}{T_1 - T_2}$ for two temperatures T_1 and T_2 close enough to each other, say, for example, $T_1 = 310$ K and $T_2 = 290$ K. We note that $e_{T_1} - e_{T_2}$ acts as a cutoff function for frequencies greater than the thermal frequency $\omega_T = \frac{2\pi c}{\lambda_T} \approx 2.5 \times 10^{14}$ rad s^{-1} ($\lambda_T \approx 7.6$ μm). The transmission factor $\mathcal{T}_L(\mathbf{k},\omega)$ thus exhibits the mode structure for the problem under study (Fig. 1) while (1) integrates the contributions of all these modes to the heat transfer, taking into account the values of their frequencies with respect to ω_T (more discussions below).

For a depth of the corrugation $a = 0$, we recover the heat transfer coefficient $h_0(L) = 0.16$ W m^{-2}K^{-1} between two gold plates separated by a distance $L = 1$ μm. For a non-null depth a, we introduce the factor of enhancement of heat transfer with respect to noncorrugated plates

$$\Omega = \frac{h(L)}{h_0(L)}. \tag{3}$$

We present in Fig. 2 the enhancement factor Ω as a function of the corrugation depth a, with the distance of closest approach $L = 1$ μm and the filling factor $p = 0.5$ kept fixed. The blue solid curve corresponds to a period $d = 1$ μm for the gratings while the red solid curve corresponds to a period $d = 2.5$ μm. The dashed curve corresponds to a period $d = 10$ μm. As the corrugations become deeper, we see a striking increase in the heat transfer coefficient. We note that the enhancement factor is largely independent of the grating period up to a corrugation depth $a \approx 1$ μm. For a period $d = 1$ μm for which the effect is more important, we get an enhancement up to a factor 10 for $a = 6$ μm. For a period $d = 2.5$ μm, the enhancement reaches nearly a factor 4 for $a = 6$ μm. For the largest period $d = 10$ μm, the enhancement still reaches nearly a factor 2 at $a = 6$ μm.

For comparison, we have shown as the dotted line in Fig. 2 the prediction of the proximity approximation (PA) which amounts to adding plane-plane heat transfer contributions, as if they were independent,

$$\Omega^{\mathrm{PA}} = p + (1-p)\frac{h_0(L+2a)}{h_0(L)}. \tag{4}$$

As expected, the PA predicts a decrease of Ω when a is increased, in complete contradiction with the exact results shown by the solid and dashed curves.

In the remainder of this Rapid Communication, we analyze the electromagnetic mode structure in order to explain the increase of the heat transfer.[17,18] To this aim, we use the scattering formula (1) and show that, as we increase the corrugation depth, some modes of the system are indeed brought to the infrared frequencies and thus are able to

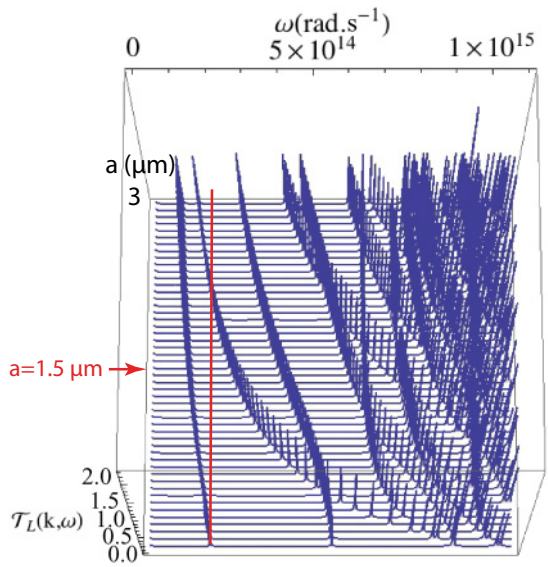

FIG. 3. (Color online) The transmission factor for two gold gratings as a function of the frequency ω and the corrugations depth a. The lower curve is for plane-plane $a = 0$ while the upper one is for a corrugations depth $a = 3$ μm. The vertical red line is the light line. The horizontal arrow at $a = 1.5$ μm shows a cut of this plot represented on Fig. 4.

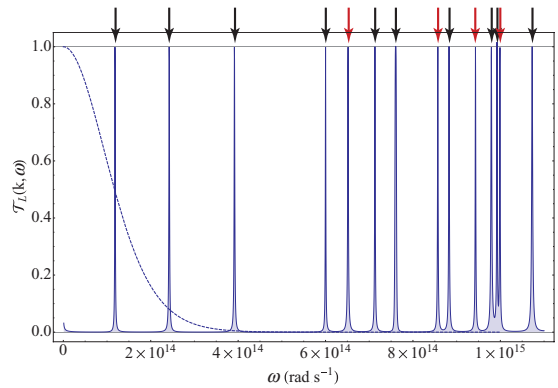

FIG. 4. (Color online) The transmission factor for two gold gratings with corrugation depth $a = 1.5$ μm as a function of frequency ω. The arrows indicate the position of the modes in a direct mode calculation [red (gray) for s polarization and black for p polarization]. The dashed curve is the function $\frac{e_{T_1}-e_{T_2}}{k_B(T_1-T_2)}$.

contribute to the heat transfer. The mode structure is described by the transmission factor $\mathcal{T}_L(\mathbf{k},\omega)$ that reaches its maximum value 1 at the resonances of the corrugated cavity. Our system is periodic so that the mode structure, distributed over the whole range of wave vectors in the absence of corrugations, now shows many branches folded in the first Brillouin zone. More precisely, there are $2(2N+1)$ branches where the factor 2 is due to the two polarizations and the factor $2N+1$ is the number of orders (or branches) used when taking into account mode coupling by diffraction on the gratings.

We represent in Fig. 3 the sum of transmission factors $\mathcal{T}_L(\mathbf{k},\omega)$ over all polarizations and all branches. It is shown as a function of the frequency ω and the depth of the corrugations a for a fixed value of the transverse wave vector $\mathbf{k} = (\frac{\pi}{2d},0)$, here chosen to be in the middle of the positive-k_x first Brillouin zone. The plot corresponds to the period $d = 2.5$ μm, which was shown as the solid curve in Fig. 2. The vertical red line represents the light line $\omega = ck_x \approx 1.88 \times 10^{14}$ rad s^{-1}.

It clearly appears in Fig. 3 that the transmission factor takes significant values only on resonances which correspond to the mode structure of the corrugated cavity. The transmission factor $\mathcal{T}_L(\mathbf{k},\omega)$ goes to a maximum value of 1 for each nondegenerate mode $(\mathbf{k},\omega)$; it can be 2 if two modes cross each other and we see one of these occurrences in the figure. The general trend is clear on the diagram: As the depth a of the corrugations is increased, new modes appear, with frequencies decreasing as a increases. When these modes enter into the thermal window $\omega \lesssim \omega_T$ they contribute more and more to the heat transfer. This explains the enhancement of the heat flux, due to the presence of additional modes in the thermal window for a deeply corrugated structure.

We now examine in more detail the nature of the modes. While varying the corrugation depth a from 0 to 3 μm we can follow the evolution of each mode. Note that, for $k_y = 0$, the polarizations $\sigma = s$ and $\sigma = p$ are not mixed (however, the computation of h takes into account all modes for which polarization mixing is important).

We show in Fig. 4 the modes calculated for a particular corrugation depth $a = 1.5$ μm indicated by the red horizontal line on Fig. 3. The position of the peaks have been confirmed through a direct mode calculation[21] of the eigenfrequencies of the structure modes obtained for p (black arrows) and s (red arrows) polarizations. In addition to the excellent agreement between the peaks of the transmission factor and the directly calculated modes (arrows on Fig. 4), direct mode calculations show the fields and, therefore, allow us to identify the first few modes. For the second p polarization and the first s polarization modes appearing at $\omega \approx 2.4 \times 10^{14}$ rad s^{-1} and $\omega \approx 6.5 \times 10^{14}$ rad s^{-1} in particular, the frequencies are largely independent upon the value of k_x, which is usually the signature of guided modes. By looking at the fields corresponding to those two modes, we indeed confirmed that the electric field is to some extent confined in the waveguides formed by the corrugations.

It is also worth discussing the shape of the resonance curve drawn by the variation of the transmission factor in the vicinity of a mode. In Fig. 5, we focus on the modes which lie inside the thermal window. In the case considered here of sharp, isolated modes, the resonance of the transmission factor shows a Lorentzian profile. We have checked that the two parameters of this profile are identified respectively to the real and imaginary parts of the complex frequency, with mode calculation of the dissipative structure defined with complex frequencies and real wave vectors.[3] This proves that the variation of the transmission factor contains all the relevant information about the mode structure. Not only the frequencies but also their finite lifetime are well described in the case considered here of lossy materials.

This discussion allows one to predict the effect of a change of the dissipation parameter γ. As this parameter is the only one to determine the widths of the peaks in the transmission factor $\mathcal{T}_L(\mathbf{k},\omega)$, one deduces that these widths vary linearly with γ. As a direct consequence of Eq. (1) and as long as

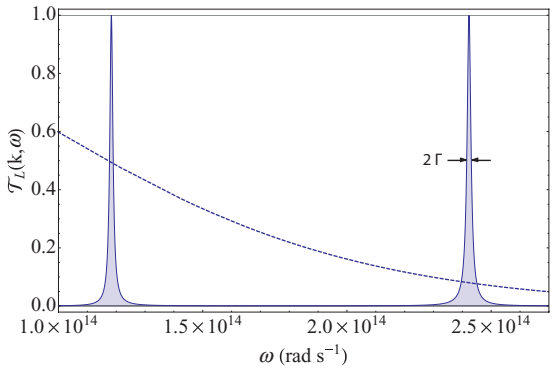

FIG. 5. (Color online) Same as Fig. 4 for the first two modes which are in the thermal window. Each peak can be fitted by a Lorentzian of resonance frequency ω_0 and half width at half maximum Γ. The dashed curve is the function $\frac{e_{T_1}-e_{T_2}}{k_B(T_1-T_2)}$.

the modes remain sharp and isolated, it follows that the heat fluxes vary in proportion of γ, so that the enhancement factor Ω, defined in Eq. (3) and drawn on Fig. 2, is independent of the dissipation parameter γ.

We have theoretically demonstrated the enhancement of the heat transfer between two nanocorrugated gold plates in comparison with flat plates with the same distance of closest approach. This enhancement is due to the presence of additional modes in the thermal frequency window contributing to the heat transfer. We have described all the relevant information about the mode structure in terms of the transmission factor $\mathcal{T}_L(\mathbf{k},\omega)$ which appears in the scattering formula for the heat flux. We have discussed the enhancement of the heat transfer in a regime where the three characteristic lengths of the problem (the distance L between the gratings, the period d of the gratings, and the height a of the corrugations) are of the same order. We stress that neither the proximity nor the effective medium approximations can work in this regime. We have in fact shown that the proximity approximation predicts a decrease of the heat transfer, in complete contradiction with the striking enhancement of the heat flux observed in the exact results.

The authors thank the ESF Research Networking Programme CASIMIR (www.casimir-network.com) for providing excellent possibilities for discussions and exchange. The research described here has been supported by Triangle de la Physique Contract No. EIEM 2010-037T. This work was carried out under the auspices of the National Nuclear Security Administration of the US Department of Energy at Los Alamos National Laboratory under Contract No. DE-AC52-06NA25396. R.G. and D.A.R.D. thank LANL and ENS, respectively, for funding their stay at these institutions, where part of this work was done.

[1] D. Polder and M. V. Hove, Phys. Rev. B **4**, 3303 (1971).
[2] A. I. Volokitin and B. N. J. Persson, Rev. Mod. Phys. **79**, 1291 (2007).
[3] K. Joulain, J.-P. Mulet, F. Marquier, R. Carminati, and J.-J. Greffet, Surf. Sci. Rep. **57**, 59 (2005).
[4] J.-P. Mulet, K. Joulain, R. Carminati, and J.-J. Greffet, Appl. Phys. Lett. **78**, 2931 (2011).
[5] S. Shen, A. Narayanaswamy, and G. Chen, Nano Lett. **9**, 2909 (2009).
[6] S.-A. Biehs, P. Ben-Abdallah, F. S. S. Rosa, K. Joulain, and J.-J. Greffet, Opt. Express **19**, A1088 (2011).
[7] S.-A. Biehs, F. S. S. Rosa, and P. Ben-Abdallah, Appl. Phys. Lett. **98**, 243102 (2011).
[8] A. W. Rodriguez, O. Ilic, P. Bermel, I. Celanovic, J. D. Joannopoulos, M. Soljačić, and S. G. Johnson, Phys. Rev. Lett. **107**, 114302 (2011).
[9] F. Marquier, C. Arnold, M. Laroche, J.-J. Greffet, and Y. Chen, Opt. Express **16**, 5305 (2008).
[10] A. Lambrecht, A. Canaguier-Durand, R. Guérout, and S. Reynaud, in *Casimir Physics*, edited by D. A. R. Dalvit *et al.*, Lecture Notes in Physics, Vol. 834 (Springer, Berlin, 2011), Chap. 4.
[11] S. J. Rahi, T. Emig, and R. L. Jaffe, in Ref. 10, Chap. 5.
[12] G. Bimonte, Phys. Rev. A **80**, 042102 (2009).
[13] R. Messina and M. Antezza, Europhys. Lett. **95**, 61002 (2011).
[14] M. Krüger, T. Emig, and M. Kardar, Phys. Rev. Lett. **106**, 210404 (2011).
[15] P. Ben-Abdallah, S.-A. Biehs, and K. Joulain, Phys. Rev. Lett. **107**, 114301 (2011).
[16] A. Lambrecht and V. N. Marachevsky, Phys. Rev. Lett. **101**, 160403 (2008).
[17] S.-A. Biehs, E. Rousseau, and J.-J. Greffet, Phys. Rev. Lett. **105**, 234301 (2010).
[18] J. B. Pendry, J. Phys. A **16**, 2161 (1983).
[19] M. G. Moharam, E. B. Grann, D. A. Pommet, and T. K. Gaylord, J. Opt. Soc. Am. A **12**, 1068 (1995).
[20] P. Lalanne and G. M. Morris, J. Opt. Soc. Am. A **13**, 779 (1996).
[21] Q. Cao, P. Lalanne, and J.-P. Hugonin, J. Opt. Soc. Am. A **19**, 335 (2002).